**Proceedings of the 2003 IEEE International Frequency Control Symposium and PDA Exhibition**
**Jointly with the 17th European Frequency and Time Forum**

# A Circuit for High Frequency Crystal Oscillators

Jun MATSUOKA, Tomio SATO, and Tsuyoshi OHSHIMA

Toyo Communication Equipment Co., Ltd.
Kanagawa-Pref. JAPAN

*Abstract*-**This paper describes a circuit for high frequency crystal oscillators using an AT-cut resonator in the UHF frequency range. This circuit can be built based on a conventional Colpitts oscillator circuit with a feedback capacitor between the collector terminal and the emitter terminal of a transistor. The new circuit has the characteristic features of low drive level and high negative resistance, while maintaining the equivalent input capacitance of the circuit. Analyzing the equivalent input impedance of the circuit clarifies the effects of the proposed circuit compared with the conventional Colpitts oscillator circuit.**

**The performance of the circuit is verified by an experimental evaluation of a voltage controlled crystal oscillator (VCXO) with a 622 MHz high frequency fundamental (HFF) crystal resonator. This VCXO offers a frequency deviation of ± 160 ppm or greater versus a control voltage change of 1.65 V ± 1.65 V, a temperature frequency stability of ± 30 ppm or less over the range from –40 °C to 85 °C, and a frequency stability of ± 5 ppm or less versus a supply voltage change of 3.3 V ± 0.3 V. A phase noise level of greater than –100 dBc/Hz at 1 kHz carrier offset frequency is demonstrated.**

## INTRODUCTION

High frequency, high stability, low noise, and wide tuning range oscillators are in demand for optical digital communication networks based on synchronous digital hierarchy (SDH) transmission system [1].

In general, crystal oscillator using an AT-cut resonator can obtain an excellent performance. However, the thickness of AT-cut resonator in the VHF/UHF frequency range becomes very thin [2], [3]. Therefore, a special attention should be made to low drive level operation in order to reduce the influence of drive level dependence and avoid breakage of the resonator.

On the other hand, there have been many studies for surface acoustic wave (SAW) oscillators in the UHF frequency range [4]-[6]. Feedback-loop oscillator circuits are particularly well suited for two-port SAW devices and generally the most commonly used configuration for SAW oscillators [5]. However, in the application of a feedback-loop oscillator circuit using AT-cut resonators in the UHF frequency range, the design is very difficult due to the low drive level operation. Accordingly, a simple oscillator circuit such as Colpitts oscillator is the most effective in maintaining the high Q of the AT-cut resonator in consideration of the low drive level operation.

As the frequency becomes higher, conventional Colpitts oscillator circuits perform at lower equivalent input capacitance. Furthermore, the equivalent parallel capacitance $C_0$ of the resonator affects the input impedance of the oscillator circuit, causing the $C_0$ to perform at very low impedance at a high oscillation frequency. Therefore, in order to apply the conventional Colpitts oscillator circuit to the UHF frequency range, it is necessary to obtain high negative resistance while maintaining the equivalent input capacitance of the circuit.

In this paper, we present a new oscillator circuit, which has the characteristic features of low drive level and high negative resistance, while maintaining the equivalent input capacitance of the circuit. This circuit can be built based on a conventional Colpitts oscillator circuit with a feedback capacitor between the collector terminal and the emitter terminal of a transistor.

First, we show the circuit configurations of both our proposed circuit and the conventional Colpitts oscillator circuit. Secondly, we analyze the input impedance of the proposed circuit compared with the conventional Colpitts oscillator circuit. Lastly, we present the experimental results of a VCXO with a 622 MHz HFF crystal resonator in order to verify the effects of the proposed circuit.

## OSCILLATOR CIRCUIT FOR UHF FUNDAMENTAL AT-CUT CRYSTAL RESONATOR

Figure 1 shows two types of oscillator circuits, which we'll develop in this paper. Fig. 1-(a) and (b) shows the circuit configurations of our proposed circuit and the conventional Colpitts oscillator circuit, respectively. We modified the circuit of Fig. 1-(b) to Fig. 1-(a) by adding a feedback capacitor $C_{ce}$ in place of $C_e$' in order to reduce the emitter voltage of the transistor. Therefore, the circuit of Fig. 1-(a) makes a low drive level operation possible, causing the proposed circuit to perform at a smaller base current due to the reduction of the emitter voltage. In order to compare with the characteristics of each circuit of Fig. 1, we set up the $C_{ce}$ and $C_e$' as a parameter.

Table 1 shows an example of the circuit parameters of Fig. 1, except $C_{ce}$ and $C_e$'. We designed the circuits (a) and (b) of Fig. 1 using the parameters of Table 1.

Figure 2 shows an example of measured crystal current characteristics for the 622 MHz crystal oscillator using the circuits of Fig. 1. The horizontal axis indicates the value of $C_{ce}$ and $C_e$', respectively. The vertical axis indicates the measured crystal current for the circuits of Fig. 1. In this figure, crystal current decreases while the value of $C_{ce}$ and $C_e$' gets larger. Furthermore, it is verified that our proposed circuit makes a low drive level operation possible compared with the conventional Colpitts oscillator circuit.

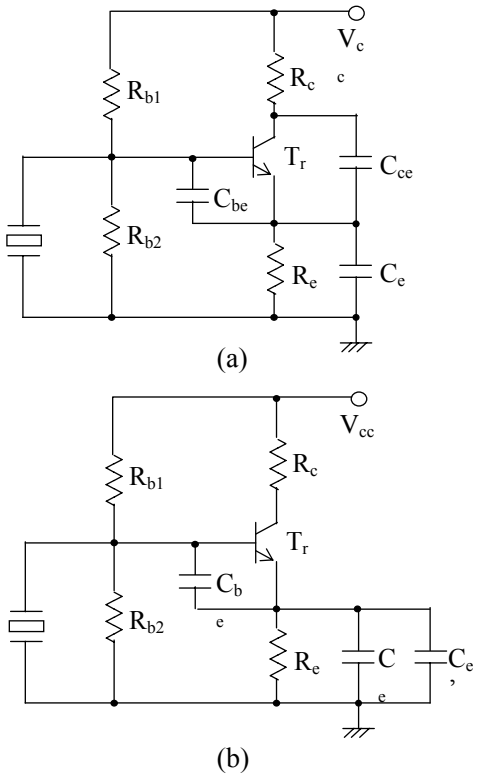


Fig. 1. Two types of oscillator circuits: (a) our proposed circuit, (b) the conventional Colpitts oscillator circuit.

TABLE 1
CIRCUIT PARAMETERS OF Fig. 1 EXCEPT $C_{ce}$ & $C_e$'

| Circuit parameter | Value |
|---|---|
| $V_{cc}$ | 3.3 V |
| $R_{b1}$ | 10 kΩ |
| $R_{b2}$ | 22 kΩ |
| $R_c$ | 47 Ω |
| $R_e$ | 100 Ω |
| $C_{be}$ | 3 pF |
| $C_e$ | 5 pF |

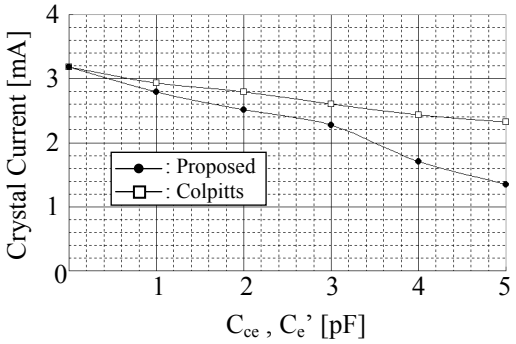


Fig. 2. An example of measured crystal current characteristics for 622 MHz crystal oscillator using the circuits of Fig. 1.

## ANALYSIS OF EQUIVALENT INPUT IMPEDANCE

Figure 3-(a) and (b) shows the simplified small signal equivalent circuits of Fig. 1-(a) and (b), respectively. The equations of equivalent input impedance of each circuit are as follows;

*Conventional Colpitts Oscillator Circuit* (Fig. 3-(b))

$$Z_b = R_b + jX_b. \tag{1}$$

$$R_b = r_1 + r_2 + g_m r_1 r_2 - \frac{g_m}{\omega^2 c_1 c_2}. \tag{2}$$

$$X_b = -\frac{1}{\omega}\left(\frac{1+g_m r_2}{c_1} + \frac{1+g_m r_1}{c_2}\right). \tag{3}$$

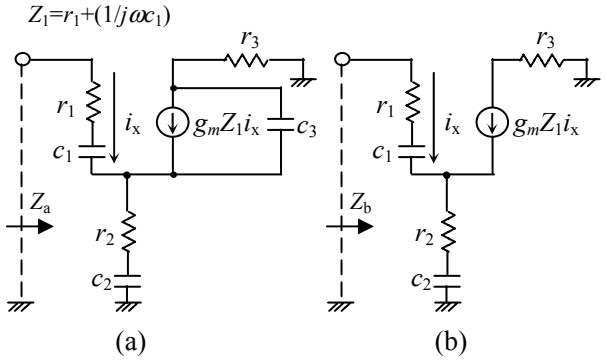


Fig. 3. The simplified small signal equivalent circuits of Fig. 1: (a) our proposed circuit, (b) the conventional Colpitts oscillator circuit.

*Our Proposed Circuit* (Fig. 3-(a))

$$Z_a = R_a + jX_a. \tag{4}$$

$$R_a = R_{a1} + R_{a2}. \tag{5}$$

$$R_{a1} = r_1 + A(r_2 + g_m r_1 r_2 - \frac{g_m}{\omega^2 c_1 c_2}). \tag{5-a}$$

$$R_{a2} = \frac{B}{\omega}(\frac{g_m r_2}{c_1} + \frac{1 + g_m r_1}{c_2}) - C(g_m r_1 r_2 - \frac{g_m}{\omega^2 c_1 c_2}) - \frac{D}{\omega}(\frac{g_m r_2}{c_1} + \frac{g_m r_1}{c_2}). \tag{5-b}$$

$$X_a = X_{a1} + X_{a2}. \tag{6}$$

$$X_{a1} = -\frac{1}{\omega c_1} - \frac{A}{\omega}(\frac{1}{c_2} + \frac{g_m r_2}{c_1} + \frac{g_m r_1}{c_2}). \tag{6-a}$$

$$X_{a2} = B(r_2 + g_m r_1 r_2 - \frac{g_m}{\omega^2 c_1 c_2}) + \frac{C}{\omega}(\frac{g_m r_2}{c_1} + \frac{g_m r_1}{c_2}) - D(g_m r_1 r_2 - \frac{g_m}{\omega^2 c_1 c_2}). \tag{6-b}$$

Where the parameters of $A$, $B$, $C$, $D$ are as follows:

$$A = \frac{(1 + \frac{c_3}{c_2}) - \omega^2 {c_3}^2 r_3 (r_2 + r_3)^2}{(1 + \frac{c_3}{c_2})^2 - \omega^2 {c_3}^2 (r_2 + r_3)^2}. \tag{7}$$

$$B = \frac{\omega c_3 (\frac{c_3}{c_2} r_3 - r_2)}{(1 + \frac{c_3}{c_2})^2 - \omega^2 {c_3}^2 (r_2 + r_3)^2}. \tag{8}$$

$$C = \frac{\omega^2 {c_3}^2 r_3 (r_2 + r_3)}{(1 + \frac{c_3}{c_2})^2 - \omega^2 {c_3}^2 (r_2 + r_3)^2}. \tag{9}$$

$$D = \frac{\omega c_3 r_3 (1 + \frac{c_3}{c_2})}{(1 + \frac{c_3}{c_2})^2 - \omega^2 {c_3}^2 (r_2 + r_3)^2}. \tag{10}$$

Where the $R_{a1}$ and $R_{a2}$ of Eq. (5) are given by Eq. (5-a) and (5-b), respectively. In addition, the equation of $R_{a1}$ is similar to Eq. (2) of the conventional Colpitts oscillator circuit, and Eq. (5) can be represented by adding the $R_{a2}$ to the $R_{a1}$. Similarly, the $X_{a1}$ and $X_{a2}$ of Eq. (6) are given by Eq. (6-a) and (6-b), respectively.

Furthermore, $A = 1$, $B = C = D = 0$, while $c_3 = 0$. That is, the equivalent input impedance of the proposed circuit can be represented by the equation of the conventional Colpitts oscillator circuit, as in the case of setting up the $C_{ce} = 0$ pF. On the basis of above equations, we analyze the effects given by the $C_{ce}$ of our proposed circuit.

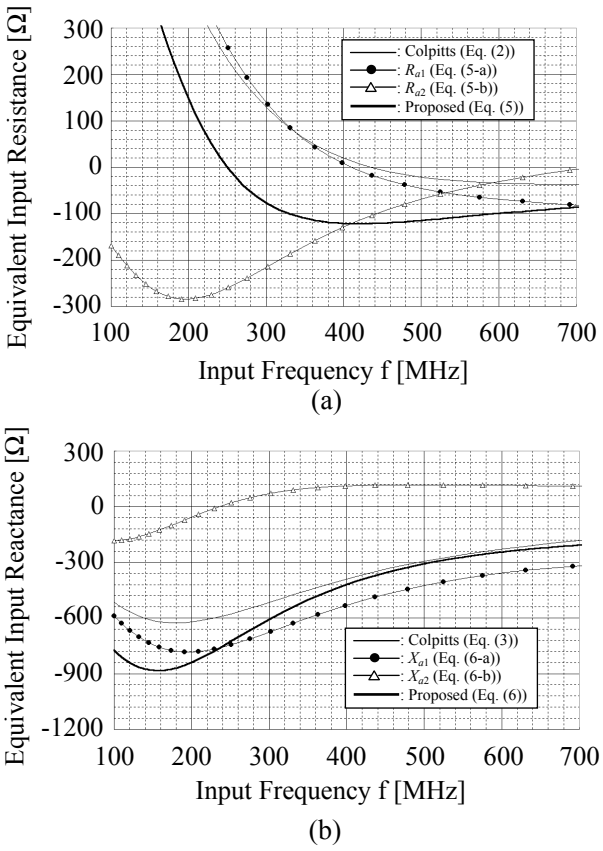


Fig. 4. An example of frequency characteristics of the equivalent input impedance analyzed by the help of the equations (1) to (10), as in the case of setting up $C_{ce} = 4$ pF and $C_e' = 0$ pF: (a) equivalent input resistance versus frequency, (b) equivalent input reactance versus frequency.

Figure 4 shows an example of frequency characteristics of the equivalent input impedance analyzed by the help of the equations (1) to (10), as in the case of setting up $C_{ce}$ = 4 pF and $C_e$' = 0 pF. The horizontal axis of Fig. 4-(a) and (b) indicates the input frequency f. The vertical axis of Fig. 4-(a) and (b) indicates the equivalent input resistance and reactance, respectively.

In Fig. 4-(a), the normal line and the bold line indicate the simulation results using Eq. (2) and (5), respectively. Moreover, the lines plotting solid circles and open triangles indicate the simulation results using Eq. (5-a) and (5-b), respectively. In this graph, the line plotting solid circles has a higher value of negative resistance compared with the normal line over a value of f = 450 MHz. In addition, the line plotting open triangles has the peak value of negative resistance at the value of f = 200 MHz. It is verified that our proposed circuit can obtain higher negative resistance by adding the characteristics of Eq. (5-b) to the Eq. (5-a), compared with the conventional Colpitts oscillator circuit.

In Fig. 4-(b), the normal line and the bold line indicate the simulation results using Eq. (3) and (6), respectively. Moreover, the lines plotting solid circles and open triangles indicate the simulation results using Eq. (6-a) and (6-b), respectively. In this graph, the line plotting solid circles has a lower value of equivalent input reactance compared with the normal line. However, the line plotting open triangles has positive values over a value of f = 240 MHz. As a result, similar values of equivalent input reactance can be obtained by using the circuits of Fig. 1 from 400 MHz to 700 MHz.

These results demonstrate that our proposed circuit has a feature of high negative resistance while maintaining the equivalent input capacitance of the circuit, compared with the conventional Colpitts oscillator circuit.

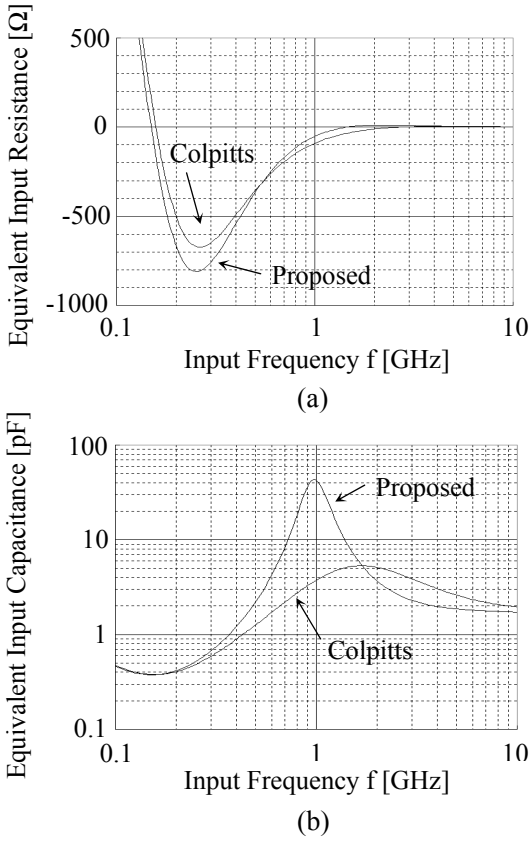


Fig. 5. An example of frequency characteristics of the equivalent input impedance analyzed by P-Spice program, as in the case of setting up $C_{ce}$ = 4 pF and $C_e$' = 4 pF: (a) equivalent input resistance versus frequency, (b) equivalent input reactance versus frequency.

## APPLICATION TO VCXO WITH 622 MHz HFF CRYSTAL RESONATOR

Figure 5 shows an example of frequency characteristics of the equivalent input impedance analyzed by P-Spice program, as in the case of setting up $C_{ce}$ = 4 pF and $C_e$' = 4 pF. The horizontal axis of Fig. 5-(a) and (b) indicates the input frequency f. The vertical axis of Fig. 5-(a) and (b) indicates the equivalent input resistance and capacitance, respectively. In this analysis, the value of negative resistance for the circuits of Fig. 1 can be approximately –250 Ω at a value of f = 600 MHz. Furthermore, our proposed circuit has a larger value of equivalent input capacitance compared with the conventional Colpitts oscillator circuit.

On the basis of above results, we built the 622 MHz VCXO and evaluated the proposed circuit. This VCXO was composed of main components such as a 622 MHz HFF crystal resonator, an output buffer (50Ω/Sine), a varactor diode and an inductor for wide tuning range. In addition, this prototype VCXO was mounted in a small package (7.0 mm x 5.0 mm x 3.0 mm).

Figure 6 to 8 shows an example of frequency deviation characteristics with a change of control voltage, temperature, and supply voltage, respectively. In these graphs, solid circles and open squares indicate measured results using the proposed circuit and the conventional Colpitts oscillator circuit, respectively.

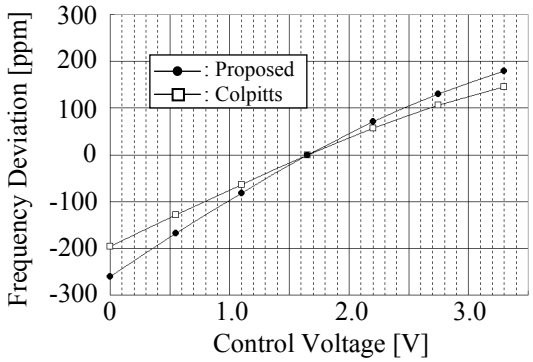


Fig. 6. The frequency deviation characteristics with a control voltage change of 1.65 V ± 1.65 V.

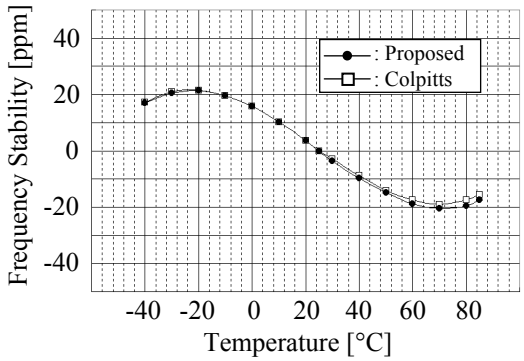


Fig. 7. The frequency deviation characteristics with a change of temperature over the range from –40 °C to 85 °C.

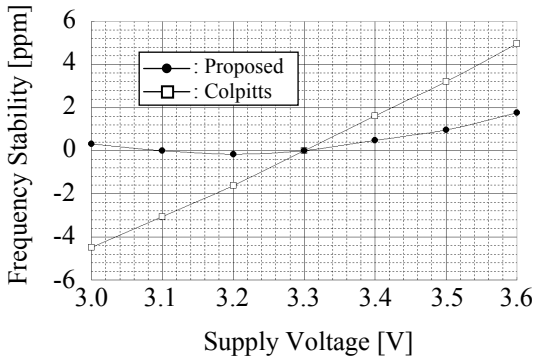


Fig. 8. The frequency deviation characteristics with a supply voltage change of 3.3 V ± 0.3 V.

Figure 6 shows the frequency deviation characteristics with a control voltage change of 1.65 V ± 1.65 V. In this figure, the proposed circuit has a wider tuning range compared with the conventional Colpitts oscillator circuit. Furthermore, VCXO using the proposed circuit offers a frequency deviation of ± 160 ppm or greater versus a control voltage change of 1.65 V ± 1.65 V.

Figure 7 shows the frequency deviation characteristics with a change of temperature over the range from -40 °C to 85 °C. In this figure, the circuits of Fig. 1 have the similar characteristics for temperature change. Furthermore, this VCXO offers a frequency stability of ± 30 ppm or less over the range from –40 °C to 85 °C.

Figure 8 shows the frequency deviation characteristics with a supply voltage change of 3.3 V ± 0.3 V. In this figure, the proposed circuit has a higher frequency stability for supply voltage change compared with the conventional Colpitts oscillator circuit. Furthermore, this VCXO offers a frequency stability of ± 5 ppm or less versus a supply voltage change of 3.3 V ± 0.3 V.

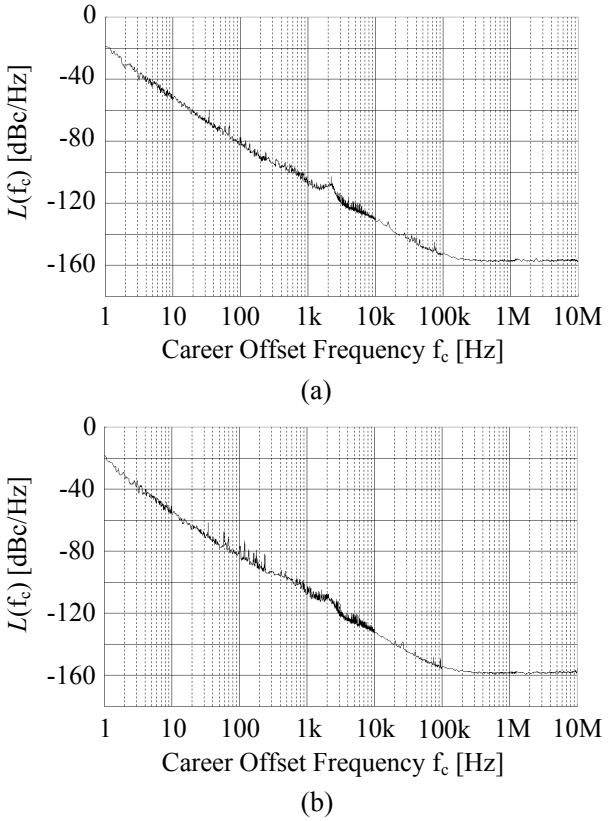


Fig. 9. An example of measured single-sideband phase noise characteristics using the circuits of Fig. 1: (a) our proposed circuit, (b) the conventional Colpitts oscillator circuit.

Figure 9-(a) and (b) shows an example of measured single-sideband phase noise characteristics using the circuits of Fig. 1. The horizontal axis of Fig. 9-(a) and (b) indicates the career offset frequency $f_c$. The vertical axis of Fig. 9-(a) and (b) indicates the single-sideband noise-to-career ratio $L(f_c)$ of the proposed circuit and the conventional Colpitts oscillator circuit, respectively. In this figure, the conventional Colpitts oscillator circuit has a lower floor noise level due to the high drive level operation compared with the proposed circuit. However, the circuits of Fig. 1 have a phase noise level of greater than -100 dBc/Hz at 1 kHz carrier offset frequency.

## CONCLUSION

First, we have proposed an oscillator circuit, which can be built based on a conventional Colpitts oscillator circuit with a feedback capacitor between the collector terminal and the emitter terminal of a transistor.

Secondly, we have shown that our proposed circuit has the characteristic features of low drive level and high negative resistance, while maintaining the equivalent input capacitance of the circuit compared with the conventional Colpitts oscillator circuit.

Finally, we have demonstrated that the 622 MHz VCXO of our proposed circuit offers the following characteristics;

1. Frequency deviation of ± 160 ppm or greater versus a control voltage change of 1.65 V ± 1.65 V.
2. Temperature frequency stability of ± 30 ppm or less over the range from –40 °C to 85 °C.
3. Frequency stability of ± 5 ppm or less versus a supply voltage change of 3.3 V ± 0.3 V.
4. Phase noise level of greater than –100 dBc/Hz at 1 kHz carrier offset frequency.

In the future, we will study a low noise and wide tuning range VCXO including a development of GHz range.

## REFERENCES


[1] O. Ishii, T. Shibata, and T. Ohshima, "High Frequency Fundamental VCXO for SDH system," in *Proc. 1996 IEEE Freq. Contr. Symp.*, 1996, pp. 714-720.

[2] H. Iwata, O. Ishii, R. Yasuike, and K. Hirama, "Suppression of Inharmonic Modes Using Peripheral Electrodes in VHF Fundamental AT-Cut Resonators," in *Proc. 2000 IEEE Freq. Contr. Symp.*, 2000, pp. 353-358.

[3] J. R. Vig, and F. L. Walls, "Fundamental Limits on the Frequency Instabilities of Quartz Crystal Oscillators," in *Proc. 1994 IEEE Freq. Contr. Symp.*, 1994, pp. 506-523.

[4] I. D. Avramov, F. L. Walls, T. E. Parker, and G. K. Montress, "Extremely Low Thermal Noise Floor, High Power Oscillators Using Surface Transverse Wave Devices," in IEEE Trans. on Ultrasonics, Ferroelectrics and Frequency Control, Vol. 43, No. 1, January, 1996, pp. 20-28.

[5] G. K. Montress, and T. E. Parker, "Design Techniques for Achieving State-of-the-art Oscillator Performance," in *Proc. 1990 IEEE Freq. Contr. Symp.*, 1990, pp. 522-535.

[6] G. K. Montress, and T. E. Parker, "Design and Performance of an Extremely Low Noise Surface Acoustic Wave Oscillator," in *Proc. 1994 IEEE Freq. Contr. Symp.*, 1994, pp. 365-373.